Effects of stratospheric variability on El Niño teleconnections

2015 Environ. Res. Lett. 10 124021

(http://iopscience.iop.org/1748-9326/10/12/124021)

Environmental Research Letters

LETTER

Effects of stratospheric variability on El Niño teleconnections

J H Richter[1], C Deser[1] and L Sun[2]

[1] Climate and Global Dynamics Laboratory, National Center for Atmospheric Research, PO Box 3000, Boulder, CO 80307, USA
[2] Cooperative Institute for Research in Environmental Sciences, University of Colorado at Boulder and NOAA Earth System Research Laboratory, Boulder, CO, USA

E-mail: jrichter@ucar.edu

Keywords: El Niño teleconnections, stratospheric variability, sudden stratospheric warmings, quasi-biennial oscillation, El Niño, El Niño impact

Supplementary material for this article is available online

OPEN ACCESS

RECEIVED
7 August 2015

REVISED
23 November 2015

ACCEPTED FOR PUBLICATION
25 November 2015

PUBLISHED
17 December 2015

Abstract

The effects of the tropical Pacific El Niño Southern Oscillation (ENSO) phenomenon are communicated to the rest of the globe via atmospheric teleconnections. Traditionally, ENSO teleconnections have been viewed as tropospheric phenomena, propagating to higher latitudes as Rossby waves. Recent studies, however, suggest an influence of the stratosphere on extra-tropical ENSO teleconnections. The stratosphere is highly variable: in the tropics, the primary mode of variability is the quasi-biennial oscillation (QBO), and in the extra-tropics sudden stratospheric warmings (SSWs) regularly perturb the mean state. Here, we conduct a 10-member ensemble of simulations with a stratosphere-resolving atmospheric general circulation model forced with the observed evolution of sea surface temperatures during 1952–2001 to examine the effects of the QBO and SSWs on the zonal-mean circulation and temperature response to El Niño, with a focus on the northern extra-tropics during winter. We find that SSWs have a larger impact than the QBO on the composite El Niño responses. During El Niño winters with SSWs, the polar stratosphere shows positive temperature anomalies that propagate downward to the surface where they are associated with increased sea-level pressure over the Arctic. During El Niño winters without SSWs, the stratosphere and upper troposphere show negative temperature anomalies but these do not reach the surface. The QBO modulates the El Niño teleconnection primarily in winters without SSWs: the negative temperature anomalies in the polar stratosphere and upper troposphere are twice as large during QBO West compared to QBO East years. In addition, El Niño winters that coincide with the QBO West phase show stronger positive sea-level pressure anomalies over the eastern Atlantic and Northern Europe than those in the QBO East phase. The results imply that the stratosphere imparts considerable variability to ENSO teleconnections.

1. Introduction

The tropical El Niño Southern Oscillation (ENSO) phenomenon provides an important source of seasonal-to-interannual climate predictability worldwide (e.g., Ropelewski and Halpert 1987, Philander 1990, Tippett and Barnston 2008). Although ENSO is generated in the tropical Indo-Pacific via coupled air-sea interactions, its effects are transmitted to the rest of the globe via large-scale atmospheric circulation teleconnection patterns excited by tropical atmospheric heating anomalies (e.g.: Horel and Wallace 1981, Trenberth *et al* 1998, Alexander *et al* 2002, and many others). A prominent example in the northern hemisphere (NH) is the intensification of the wintertime Aleutian Low pressure system in response to the warm phase of ENSO, which brings above normal temperatures and precipitation to parts of western North America. The response of the Aleutian Low and associated downstream centers-of-action of the Pacific-North American (PNA) teleconnection pattern (Wallace and Gutzler 1981, Quadrelli and Wallace 2004) to ENSO is caused by tropospheric Rossby waves forced by anomalous deep convection in the

tropical Indo-Pacific, with subsequent feedbacks from transient-eddy momentum fluxes (e.g.: Trenberth *et al* 1998, Held *et al* 2002, Branstator 2003). Similar mechanisms underlie ENSO teleconnections in other areas, including the southern hemisphere (Jin and Kirtman 2009).

In addition to ENSO, numerous studies have shown that the stratospheric polar vortex can influence the extra-tropical tropospheric circulation, particularly in the Arctic and North Atlantic sectors (Baldwin and Dunkerton 2001, Thompson and Wallace 2001). For example, a weak polar vortex is often accompanied by stratospheric sudden warming (SSW) events during which the winds reverse from easterly to westerly and the polar stratosphere warms by tens of degrees within a few days (Chartlon and Polvani 2007). SSWs may in turn influence the tropospheric circulation by inducing the negative phase of the Northern Annular Mode or North Atlantic Oscillation (NAO) for up to 60 days following an event, providing a source of tropospheric predictability (Baldwin and Dunkerton 2001, Gerber *et al* 2009, Sigmond *et al* 2013, Tripathi *et al* 2014, Scaife *et al* 2015). The precise mechanisms for this linkage are complex and still not fully understood, but involve stratospheric 'downward control' and tropospheric eddy momentum feedback (see Kidston *et al* 2015 and references therein). The quasi-biennial oscillation (QBO), a prominent zonal wind oscillation in the tropical lower stratosphere with an average period of 28 months (Baldwin *et al* 2001), can modulate the strength of the stratospheric polar vortex and thus consequently affect the tropospheric circulation (Thompson and Wallace 2001, Scaife *et al* 2014). As shown in the early observational studies of Holton and Tan (1980, 1982), when tropical zonal winds at 50 hPa are westerly (e.g., west phase of the QBO), the stratospheric polar night jet is stronger than when the QBO is in its east phase. An overview of the generation mechanisms, modeling, and impacts of the QBO is provided in Baldwin *et al* (2001).

Because ENSO, SSWs and the QBO independently affect the extra-tropical tropospheric circulation, El Niño events that coincide with the occurrence of an SSW or with a particular phase of the QBO may be accompanied by a different pattern of circulation anomalies than El Niño events in which SSWs are absent or the QBO is in a neutral phase. For example, Ineson and Scaife (2009) showed that the response to El Niño is amplified during winters with SSWs compared to winters without SSWs based on simulations with the vertically-extended version of the Met Office Hadley Centre climate model, HadGAM1. Based on close analysis of observations, Ineson and Scaife (2009) suggested distinct tropospheric and stratospheric pathways by which ENSO can influence the northern extra-tropics. According to Butler *et al* (2014), the stratospheric teleconnection is primarily via SSWs. Recently, Iza and Calvo (2015) noted that in the observational record, the stratospheric and upper tropospheric polar vortex warms and weakens only during El Niño winters with SSWs and cools and strengthens during El Niño winters without SSWs. Domeisen *et al* (2015) found that 500 hPa geopotential height anomalies for El Niño winters resemble a typical NAO pattern only for winters with SSWs in the Max Plank Institute-Earth System Model (MPI-ESM) seasonal prediction system.

The representation of the QBO has been a challenge for many general circulation models (GCMs). Calvo *et al* (2009) used the Middle Atmosphere ECHAM5 model to examine the effect of the QBO on the 80°N zonal mean temperature and 60°N zonal wind response to a single strong El Niño event. They found that the onset of the stratospheric extra-tropical anomalies associated with El Niño is delayed when the QBO is in its westerly phase compared to its easterly phase. Garfinkel and Hartman (2010) examined the influence of the QBO on El Niño teleconnections over the North Pacific in reanalysis data and simulations with the Whole Atmosphere Community Climate Model, a model with a well-resolved stratosphere and a lid near 140 km. They found a stronger El Niño teleconnection during the westerly QBO phase as compared to the easterly phase. They suggested that the QBO has an influence on tropospheric wave propagation, and hence on the teleconnection pattern.

In this study, we examine the effects of both the QBO and SSWs on the zonal-mean NH winter atmospheric circulation response to El Niño events using a new, higher-top configuration of the Community Atmosphere Model, version 5 (CAM5). This version of the model produces an internally-generated QBO as well as a realistic frequency of occurrence of SSWs. Our results are based on a 10-member ensemble of simulations forced with the observed evolution of sea surface temperatures during 1952–2001. The large sample size allows for a robust assessment of the influence of the QBO and SSWs on the response to El Niño. Note that this study does not attempt to address causality among ENSO, QBO and SSWs. Rather, its purpose is to highlight how the superposition of these phenomena in various combinations contributes to a wide range of El Niño teleconnections.

2. Model description and methods

We use a new version of CAM5 (Richter *et al* 2014a, 2014b) that has 46 vertical levels and a model top at 0.3 hPa instead of the standard configuration (Neale *et al* 2012) with 30 levels and a model top at ~2 hPa (see figure S1 for details of the vertical grid). We use a spectral element dynamical core (Dennis *et al* 2012) with a horizontal resolution of approximately 100 km. The 46-level version of CAM5, hereafter referred to as 46LCAM5, includes the Richter *et al* (2010) parameterization of non-orographic

gravity waves, similar to that in Richter *et al* (2014a). The convective gravity wave efficiency was adjusted so as to produce a realistic QBO period in the lower stratosphere.

We conducted a 10-member ensemble of simulations with 46LCAM5 for the period 1952–2001, using the observed evolution of global monthly sea surface temperatures and sea ice conditions as lower boundary conditions from Hurrell *et al* (2008) and observed external radiative forcings (solar, greenhouse gases, volcanoes, and aerosols). The first 6 ensemble members were initialized with the same wind profile in the QBO neutral phase and small (order 10^{-14} K) perturbations to the initial temperature profile. The additional four ensemble members start with a tropical zonal wind profile in the easterly QBO phase (plus small perturbations to the temperature profile) in order to change the relationship between the phase of ENSO and QBO in the various ensemble members. This experimental design allows us to study El Niño teleconnections subject to different phases of the QBO; however, we note that the simulated pairings between individual El Niño events and QBO phase may not be as observed.

We define El Niño events based on years when the December value of the monthly Niño 3.4 SST anomaly exceeds 1 standard deviation after smoothing with a 3-point binomial filter following Deser *et al* (2010). With this criterion, 8 El Niño winters are identified during our period of analysis: 1957/58, 1965/66, 1972/73, 1982/83, 1986/87, 1991/92, 1994/95, and 1997/98.

Following Butler *et al* (2014), we identify an SSW when the zonal-mean westerly wind at 10 hPa and 60° N reverses sign during the months November through March. Zonal-mean winds are required to return to westerly for 20 consecutive days before a new SSW event can be defined. In our SSW counts, we do not include final warmings, in which the zonal-mean zonal wind becomes easterly and does not return to westerly for at least 10 consecutive days before 30 April.

We define westerly (easterly) QBO winters as those in which the December-February (DJF) average zonal-mean equatorial (2°S–2°N) zonal wind at 30 hPa is >2.5 m s^{-1} (< -2.5 m s^{-1}). Using a stricter definition of the QBO (± 5 m s^{-1} threshold) yields similar results (not shown).

We form composites over all 8 El Niño winters, and also sub-divide these composites according to the phase of the QBO and occurrence of SSWs. The significance of the results is assessed using a student-t test, using the mean and standard deviation of the events that make up each composite and comparing these with the mean and standard deviation of all years. We compare the model results to zonal-mean zonal winds and temperatures from the ERA-40 Reanalysis (ERA-40; Uppala *et al* 2005) and sea level pressure (SLP) from the 20th Century Reanalysis version 2 (20CR; Compo *et al* 2011).

3. SSWs and QBO in CAM5

Realistic simulation of SSWs and the QBO is critical to studying their influence on tropospheric climate. The frequency of occurrence of SSWs based on the NCAR/NCEP Reanalysis (Kalnay *et al* 1996), for which reliable stratospheric data are available starting in 1957, is approximately 0.6 per year (Charlton *et al* 2007). The SSW frequency averaged over the 10-member 46LCAM5 ensemble is also 0.6 per year. Another important aspect of SSWs is their seasonal distribution. The frequency of observed SSWs peaks in January and February (1.5 per decade; figure S2). The mean $\pm$ one standard deviation of SSW frequency in the 46LCAM5 ensemble encompasses the observations in each winter month (November–March), indicating that the model simulates a realistic seasonal distribution. On average, the simulated SSW frequency is slightly higher in November, December and March and slightly smaller in January and February compared to observations (figure S2).

The internally-generated QBO in 46LCAM5 exhibits an average period of 27 months, very similar to the observed mean of 28 months (figure S3). The amplitude of the westerly phase of the QBO in 46LCAM5 is realistic (15–20 m s^{-1}), but the easterly phase is weaker than observed (-20 to -28 m s^{-1} compared to -25 to -35 m s^{-1} at 20 hPa: figure S3).

4. El Niño teleconnections

4.1. Mean response and variability

Following previous studies (Manzini *et al* 2006 and Calvo *et al* 2009), figure 1 shows the observed and simulated El Niño composites of zonal mean anomalies of temperature at 80°N (hereafter T80N) and zonal wind at 60°N (hereafter U60N) from October through April, between 1000 and 1 hPa. Note that observations are based on 8 events, while the model results are based on 80 events obtained by combining all 10 simulations. In observations, El Niño elicits a warming of the polar vortex that peaks in February with a maximum amplitude of approximately 10 K (figure 1(a)). The polar stratospheric warming is associated with a weakening of the midlatitude jet by up to 17 m s^{-1} (figure 1(b)). The warming of the polar vortex descends into the lower stratosphere and troposphere with time, arriving at the surface in March. The stratospheric signals are significant at the 95% level, whereas those in the troposphere are not. The El Niño composite in the 46LCAM5 ensemble based on all 80 events shows similar features as in ERA-40, but with weaker amplitude and stronger connection to the surface (figures 1(c) and (d)). In addition, the model response exhibits higher statistical significance

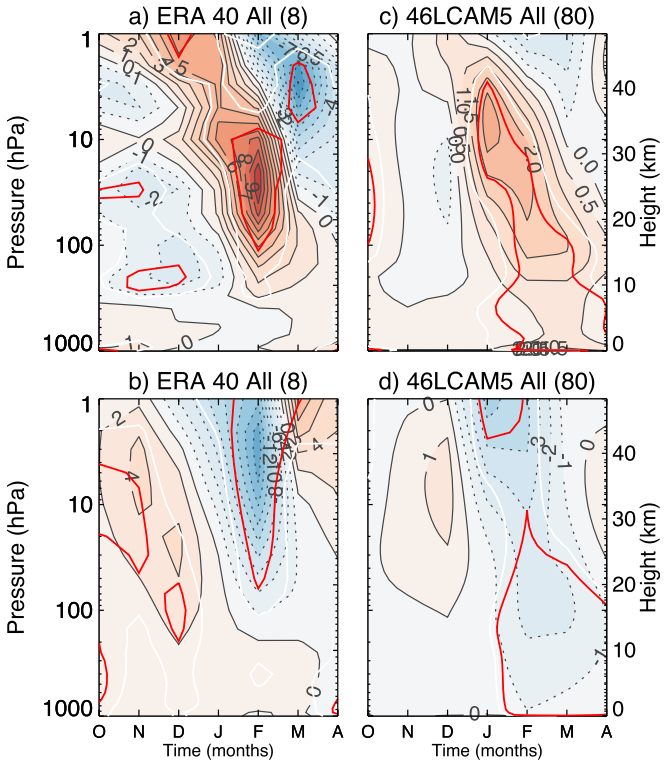

Figure 1. El Niño composites of zonal mean anomalies of temperature at 80°N (top) and zonal wind at 60°N (bottom) from October through April for ERA-40 (left column) and the 46LCAM5 10-member ensemble (right column). The number of El Niño events included in each panel's average is depicted in parenthesis in the title of each panel. Contour interval for temperature anomalies is 1.0 K for ERA-40 and 0.5 K for 46LCAM5. Contour interval for zonal wind anomalies is 2.0 m s^{-1} for ERA-40 and 1.0 m s^{-1} for 46LCAM5. The statistical significance of the signal based on the student t-test at the 85% and 95% levels are depicted by white and red lines, respectively.

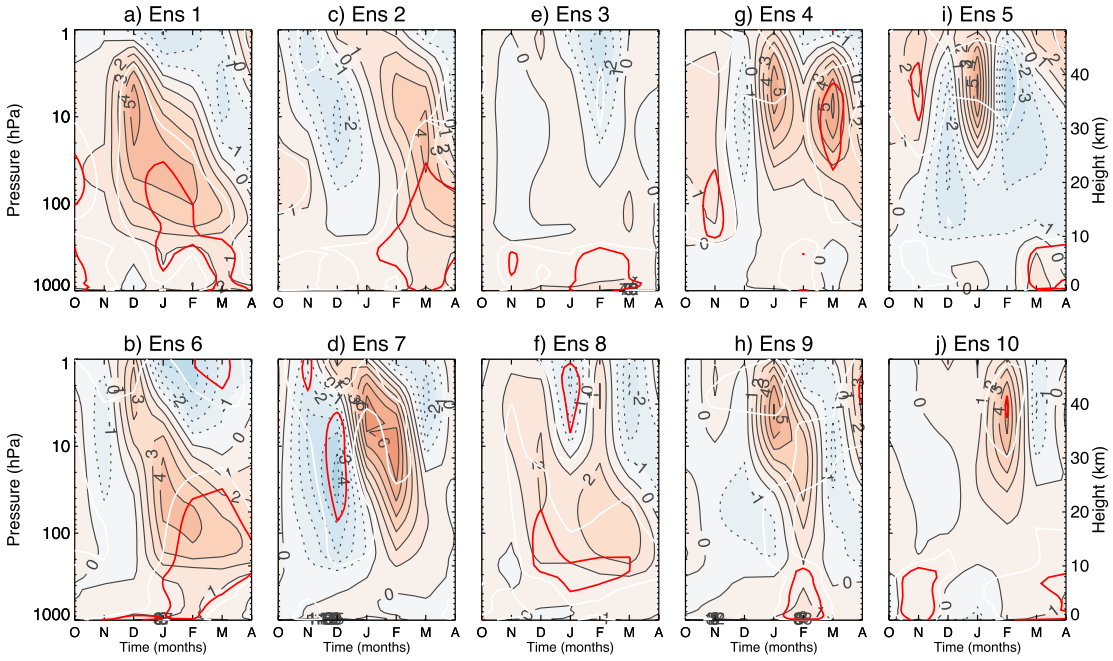

Figure 2. As in figure 1(c) but for each of the 10 46LCAM5 ensemble members. Contour interval is 1.0 K. Statistical significance of the signal based on the student t-test at the 85% and 95% levels are depicted by the white and red lines, respectively.

(>95%) throughout the stratosphere and troposphere compared to observations, due mainly to the larger sample size. In the 46LCAM5 ensemble mean, the maximum T80N is ~2.5 K compared to 10 K in ERA-40, and the maximum U60N is 4 m s^{-1} compared to 17 m s^{-1} in ERA-40.

An immediate conclusion that might be drawn from this comparison is that 46LCAM5 underestimates the magnitude of the extra-tropical El Niño response in the stratosphere, and overestimates the downward connection to the surface. However, it is important to consider the variability of the El Niño response across the ensemble members, since observations contain the equivalent of one realization of 46LCAM5. Figure 2 shows that there is considerable diversity in the response across the 10 ensemble members. Some (1, 2, 6, 7, and 9) show clear evidence of downward propagation of positive T80N from the stratosphere to the troposphere albeit with differences in magnitude and timing, while others (3, 5, 10) lack coherent warming and downward influence. Similar results are found for U60N (not shown). These results suggest that a downward propagating T80N (or U60N) signal averaged over a sample of 8 events during 1957–2001 is not a universal response to El Niño, at least according to 46LCAM5. Of all the ensemble members, number 7 shows the closest match to observations in terms of T80 pattern and amplitude (and U60N; not shown), indicating that the model is capable of producing approximately the 'correct' signal; however the large spread across the ensemble members suggests that this response is not necessarily expected in any single realization. We speculate that the overall weaker-than-observed El Niño response in 46LCAM5 might also be partially caused by the deficient amplitude of the resolved tropical wave spectrum related to the convection parameterization (Zhang and McFarlane 1995).

The extra-tropical El Niño response in the Middle Atmosphere ECHAM5 model shown by Calvo *et al* (2009) is nearly three times stronger than in 46LCAM5. However, the El Niño response in Calvo *et al* (2009) was based on a single, very strong El Niño event (1997–1998). We find a similar amplitude response in the 46LCAM5 when we restrict our El Niño composite to the two strongest events (1982–83 and 1997–1998), with a maximum value of T80N (U60N) in the stratosphere of 8 K (-14 m s^{-1}) in January, very similar to the values reported in Calvo *et al* (2009). This demonstrates that the strength of the stratospheric response is modulated by the strength of the El Niño event, and that 46LCAM5 produces an El Niño response consistent with previous studies.

The 8 El Niño events that make up our composites are based on a 1 standard deviation threshold of the Niño 3.4 Index (recall section 2). We have repeated our analysis using a more lenient criterion (a 0.5 °C threshold of the Nino3.4 index for 5 consecutive seasons following Butler *et al* 2014) and find generally similar results, although the timing of the stratospheric T80N anomalies is 1 to 2 months earlier for weak events compared to strong events (not shown). This may be due to the fact that the Niño 3.4 SST anomalies tend to peak earlier during weak events compared to strong events (October to November versus December to January: not shown), but further work is needed to establish causality.

4.2. Influence of SSWs

Here we examine the sensitivity of the composite El Niño teleconnections to SSW occurrence by dividing the El Niño winters into those that contain at least one SSW and those without any SSWs. Of the 8 El Niño winters sampled in the observational record, 4 were accompanied by at least one SSW and 4 had no SSWs. The observed composite of El Niño winters with SSWs shows a positive T80N propagating from the stratosphere to the upper troposphere between January and March, followed by a similar downward-propagating negative T80N signal (figure 3(a)). In contrast, during winters without SSWs, the warming is confined near 10 hPa during January and February, accompanied by cooling throughout most of the lower stratosphere in the early part of the winter and in the upper troposphere over the entire winter (figure 3(b)). Of the 80 El Niño winters sampled in the 46LCAM5 ensemble, 46 were accompanied by at least one SSW and 34 had no SSW occurrences. Overall, the 46LCAM5 composites with and without SSWs are similar to their observed counterparts (figure 3). For example, El Niño winters with SSWs show evidence of downward propagation of T80N from the stratosphere to the troposphere beginning in January (figure 3(c)). This downward propagation extends all the way to the surface in the model, unlike observations, with maximum and statistically significant warming at 1000 hPa in March (figure 3(c)). El Niño winters without SSWs in the model show cooling in the lower stratosphere and upper troposphere in early winter, persisting into late winter in the upper troposphere, similar to observations (figure 3(d)). Unlike observations, the simulated cooling is followed in January by warming near 2 hPa that subsequently descends into the troposphere as spring progresses; the observed warming maximum at 10 hPa in January is not simulated by the model. The differences in the composite of El Niño events with and without SSWs are also clear from the U60N anomalies as shown in figure S4.

4.3. Influence of the QBO

Due to the substantial influence of SSWs on El Niño teleconnections, we consider the influence of the QBO separately for winters with and without SSWs. The overall structure of T80N during winters with SSWs is similar during QBOE (12 events; figure 3(e)) and QBOW (26 events; figure 3(g)); however, the timing of individual features differs slightly. During QBOE years, stratospheric T80N starts increasing in December reaching its maximum in the stratosphere near 10 hPa in January, whereas during QBOW years T80N increases beginning in January and reaches it's maximum near 10 hPa in February. These differences in T80N between QBOW and QBOE are significant at

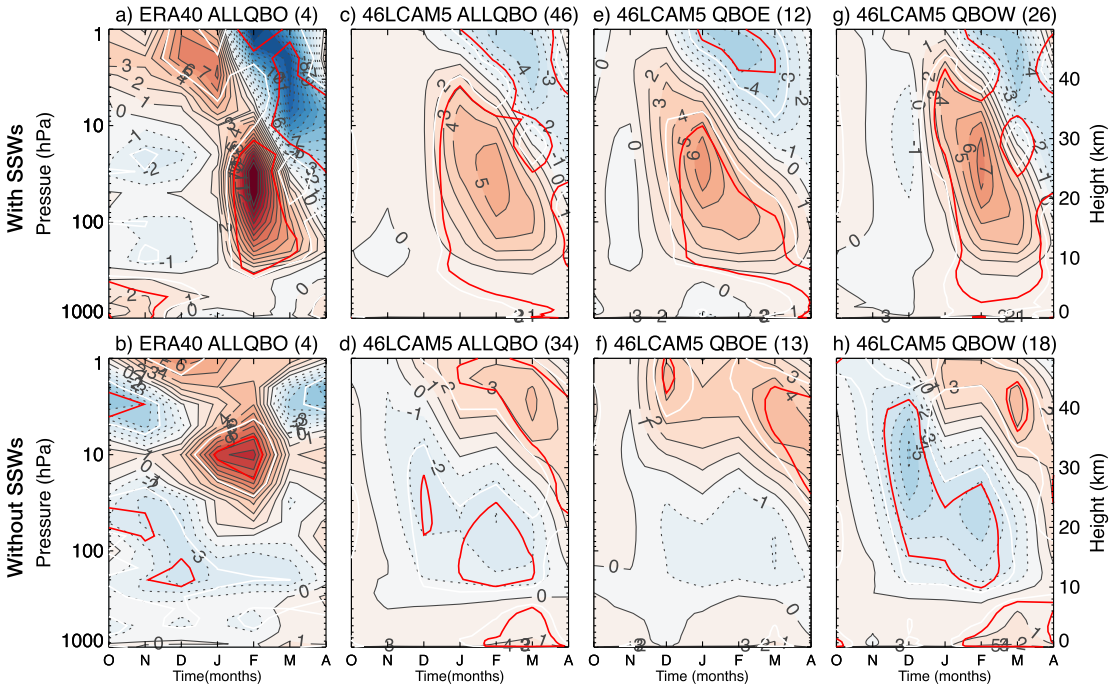

Figure 3. El Niño composites of zonal mean temperature anomalies at 80°N from October through April for ERA40 (first column) and 46LCAM5 simulations (remaining columns). Top panels show composites of winters with SSWs whereas the bottom panels show winters without SSWs. The first two columns show an average over all QBO phases, whereas columns 3 and 4 show QBOE and QBOW phases, respectively. Statistical significance of the signal based on the student t-test at the 85% and 95% levels are depicted by the white and red lines, respectively.

the 85% level per the student-t test (figure S5(a)). Similar differences in timing are also evident in the U60N responses between QBOE and QBOW years (figures S4(e), S4(g)).

The phase of the QBO has a stronger influence on the structure of the T80N and U60N responses to El Niño during winters without SSWs compared to winters with SSWs (figures 3(f), (h), and S5(b)). During El Niño winters without SSWs, between November and April, T80N is weakly negative throughout the lower stratosphere (up to ∼10 hPa) during QBOE (13 events; figure 3(f)), and is positive above 10 hPa. During QBOW El Niño winters without SSWs (18 events; figure 3(h)), T80N is also negative, but much stronger in magnitude, with a cooling of −5 K in December near 10 hPa, that descends into the lower stratosphere by February/March. U60N during QBOE is generally 2 m s^{-1} or less throughout the stratosphere between October and April (figure S4(f)), whereas it is between 2 and 8 m s^{-1} in the stratosphere between November and March during QBOW (figure S4(h)). In addition to the differences in the stratosphere between QBOE and QBOW years, El Niño winters without SSWs show a statistically significant 1 K T80N signal near the surface between January and March during QBOW years (figure 3(h)), a feature that is not present during QBOE years (figure 3(f)). This warming is associated with the weakening of U60N in the mid-troposphere by up to 2 m s^{-1} in March during QBOW, significant at the 95% level (figure S4(h)).

In order to ensure that the differences between QBOE and QBOW signals shown in figure 3 are indeed a result of the QBO and not a result of sampling different El Niño events, we have repeated our analysis using the same set of El Niño events for both QBO phases and found similar results (not shown).

Figure 3 highlights the importance of examining the effects of the QBO in El Niño winters with and without SSWs separately. Although Calvo *et al* (2009) examined the influence of the QBO on T80N during the 1997 to 1998 El Niño event using a large ensemble of simulations, they did not stratify their results according to the occurrence of SSWs, and hence their results cannot be directly compared to ours.

To summarize, our results suggest that the downward propagation of positive T80N (and negative U60N) anomalies from the stratosphere to the troposphere occur primarily in El Niño winters with SSWs as opposed to El Niño winters without SSWs with a slight modulation in timing by the QBO (figure 3). However, during El Niño winters without SSWs, the QBO has a clear influence: during QBOW the stratospheric vortex is much cooler and stronger especially between November and January as compared to QBOE winters.

Several previous studies have investigated interactions between QBO, ENSO and stratospheric conditions. For example, Garfinkel and Hartmann (2007) found that the polar vortex is stronger in QBOW years compared to QBOE years during La Nina and neutral

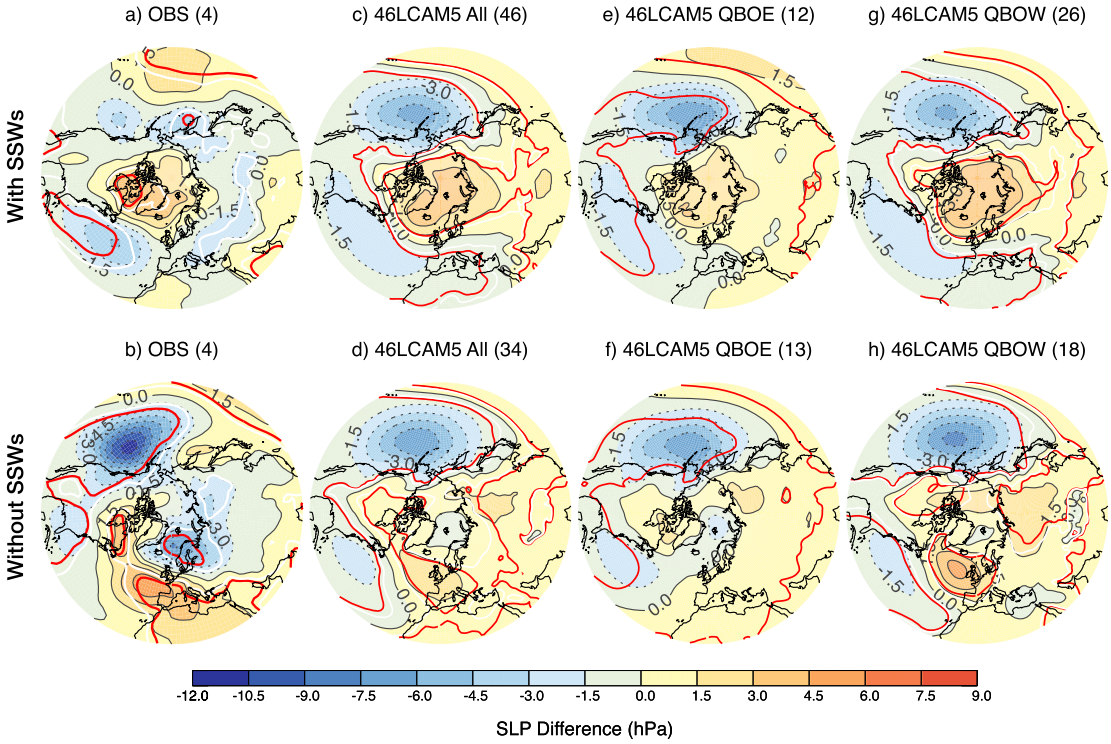

Figure 4. El Niño composites of sea level pressure anomalies for January–March based on 20th Century Reanalysis (first column) and 46LCAM5 (remaining columns). Top panels show composites of winters with SSWs whereas the bottom panels show winters without SSWs. The first two columns show an average over all QBO phases, whereas columns 3 and 4 show El Niño QBOE and QBOW phases, respectively. Number of El Niño events included in the composite is noted in parenthesis next to the panel labels. Contour interval is 1.5 hPa. Statistical significance of the signal based on the student t-test at the 85% and 95% levels are depicted by the white and red lines, respectively.

ENSO conditions, but not during El Niño conditions. This nonlinearity was further explored in Garfinkel and Hartmann (2008), who showed that when El Niño and the QBOE phase occur together, the teleconnection pattern does not resemble the PNA pattern, and therefore the upward wave propagation into the stratosphere is not enhanced. In our study we do not examine the mechanisms behind the interactions of the QBO and El Niño teleconnections. Possible mechanisms were proposed by Garfinkel *et al* 2010 and Garfinkel and Hartmann (2010, 2011a, b). However, our study strongly suggests that the interactions of El Niño and QBO are very different for winters with and those without SSWs, and hence should be examined separately.

4.4. Surface Teleconnections

Figure 4 shows the corresponding spatial distributions of SLP anomalies during January–March (JFM) based on observations (20th Century Reanalysis) and 46LCAM5. The JFM season was chosen based on when the zonal-mean T80 and U60 signals reach the surface (recall figures 1 and 3). In observations, El Niño JFM winters with SSWs show a significant negative NAO response, with positive SLP anomalies in the Arctic and negative anomalies over the North Atlantic (maximum amplitudes ∼4.5 hPa in both regions; figure 4(a)). Surprisingly, there is little signal over the Aleutian Low region in the 4-event composite, although 2 of the individual winters do show a significant deepening of the Aleutian Low (not shown). Note that the 4 El Niño events with SSWs (1957/58, 1965/66, 1972/73, 1986/87) are generally weaker than those without SSWs (1982/83, 1991/92, 1994/95, 1997/98), which may explain the lack of a significant Aleutian Low response in the former compared to the latter. Farther south, the western North Pacific shows significant positive SLP anomalies, as expected for El Niño events. The observed El Niño JFM composite for winters without SSWs shows a strong and significant deepening of the Aleutian Low, and a significant positive NAO-like response in the far eastern Atlantic (figure 4(b)).

The model also shows differences in the JFM SLP anomaly pattern between winters with SSWs (46 events over the 10 ensemble members) and those without SSWs (34 events over the 10 ensemble members) that resemble those in nature. During winters with SSWs, 46LCAM5 shows positive SLP anomalies in the Arctic (maximum amplitude ∼4 hPa) coupled with negative anomalies over the North Atlantic and North Pacific, all of which are statistically significant at the 95% confidence level (figure 4(b)). During winters without SSWs, the model shows a weak response in the Arctic and Atlantic sectors, but the spatial pattern is not unlike that found in observations (figure 4(d)).

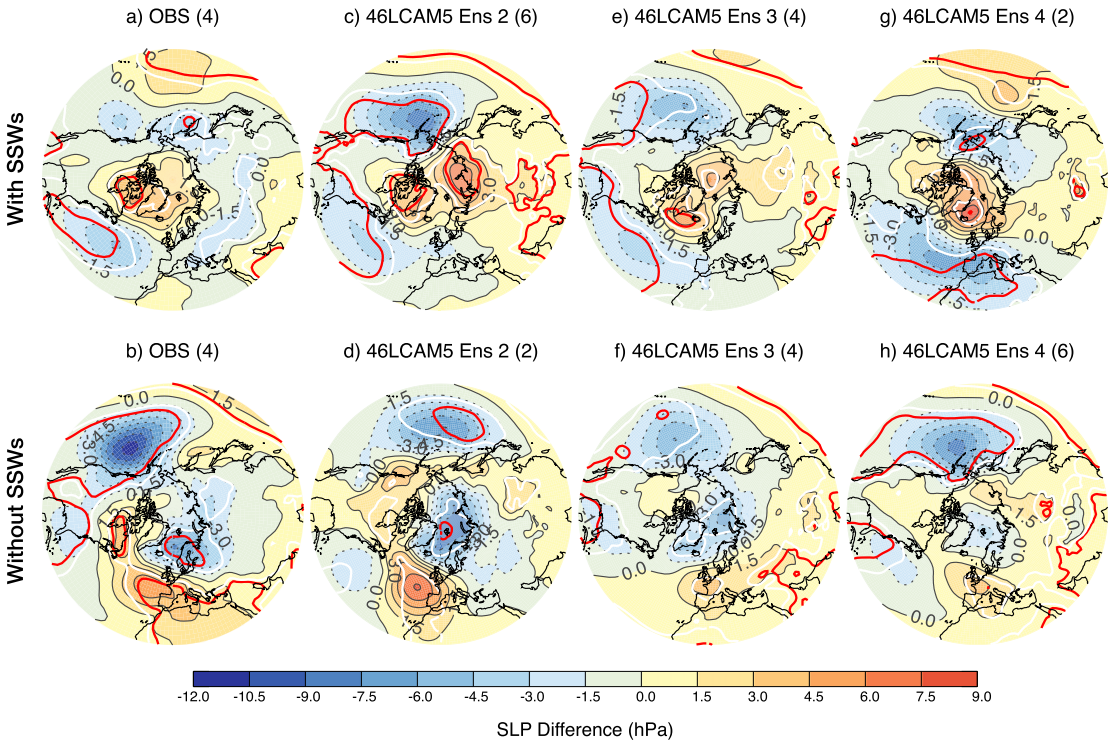

Figure 5. El Niño composites of sea level pressure anomalies for January–March based 20th Century Reanalysis (first column) and three individual ensemble members of 46LCAM5 (remaining columns). Top panels show composites of winters with SSWs whereas the bottom panels show winters without SSWs. Number of El Niño events included in the average is noted in parenthesis next to the panel labels. Contour interval is 1.5 hPa. Statistical significance of the signal based on the student t-test at the 85% and 95% levels are depicted by the white and red lines, respectively.

The weakness of the NAO-like pattern in figures 4(c) and (d) is partly due to the large variability of the ENSO response in 46LCAM5. Figure 5 compares the JFM SLP anomaly pattern for observations to three individual ensemble members of 46LCAM5. These three particular ensemble members show a NAO-like pattern, with positive SLP anomalies over Europe and East Atlantic, and negative anomalies over the Arctic during winters without SSWs, and an opposite pattern during winters with SSWs. The surface ENSO response in these three selected ensemble members is very similar to observations suggesting that the model reproduces the observed ENSO teleconnections; however only half of our ensemble members show this pattern, further underlining the role of sampling variability.

It is interesting to note that the observed El Niño composite with SSWs shows a small but significant negative SLP response in the far northwestern subpolar Pacific, unlike the observed El Niño composite without SSWs, which is dominated by a strong deepening of the Aleutian Low (figures 5(a) and (b), respectively). This is consistent with Garfinkel *et al* (2012), who found that 500 hPa geopotential height variability in the northwestern subpolar Pacific is crucially important for whether El Niño leads to an SSW or not. The model ensemble members do not consistently show this result, although member number 4 comes closest to the observed SLP patterns in El Niño years with SSWs and those without SSWs (figures 5(g) and (h), respectively).

The phase of the QBO also influences the SLP response. During winters with SSWs these effects are small and statistically insignificant as shown in figure S6 (a). Consistent with the stronger tropospheric response shown in figure 3(h), the influence of the QBO is larger during El Niño winters without SSWs. In particular, the positive anomaly center west of the UK is significantly stronger in QBOW compared to QBOE years (figures 4(f) and (h) and figure S6(b)). The SLP El Niño response is also strengthened over Northern Eurasia in QBOW years as compared to QBOE years. It is worth noting that out of the 4 observed El Niño winters without SSWs, two were in the QBOW phase (with one each in the QBO neutral and QBOE phases).

5. Discussion and conclusions

We have examined the northern hemisphere extratropical stratospheric and tropospheric response to El Niño using a 10-member ensemble of simulations for the period 1952–2001 based on 46LCAM5, a model that produces an internally-generated QBO and has a realistic frequency and seasonal distribution of SSWs. Overall, the simulated response to the composite of 80 El Niño events (8 events × 10 simulations) resembles the observed response based on 8 events, with a warmer

and weaker stratospheric vortex in January that propagates down to the troposphere, arriving at the surface between February and March. However, individual ensemble members show considerable diversity in their composite El Niño responses. For example, only 6 out of 10 ensemble members show downward propagation of a warm and weak vortex signal from the stratosphere to the troposphere in response to El Niño, and the timing and amplitude of this response is highly variable. Thus, direct comparison of the El Niño response in the model and observations must account for both the forced signal and internal atmospheric variability (e.g., sampling variability).

We find that the occurrence of SSWs, as compared to the phase of the QBO, has a more pronounced effect on the simulated extra-tropical El Niño response. For example, during El Niño winters with SSWs there is a clear downward propagation of positive T80N and negative U60N from the stratosphere to the lower troposphere between January and March, whereas in winters without SSWs, the stratosphere is cooler between November and March and does not appear to influence the lower troposphere. These findings are in agreement with the observational study of Butler *et al* (2014) who attribute the stratospheric pathway of El Niño teleconnections to SSWs, as well as the modeling study of Domeisen *et al* (2015) who showed that El Niño teleconnections were different for winters with and without SSWs during the period 1981–2002.

We find that the phase of the QBO has a small, but noticeable, effect during El Niño winters with SSWs. In particular, T80N reaches a maximum in stratosphere in January in QBOE winters, and in February in QBOW winters. The descent of the T80N anomaly to the troposphere is faster in QBOW winters as compared to QBOE winters. Calvo *et al* (2009) found that T80N anomalies persisted longer during QBOW as compared to QBOE, however they only studied the response to the strong 1997/1998 El Niño event and did not separate their ensemble members into winters with and without SSWs, hence the results are not directly comparable.

We find that the QBO primarily influences El Niño teleconnections during winters without SSWs. Specifically, the stratospheric and upper tropospheric cooling between November and March at 80°N and strengthening of the stratospheric jet at 60°N is twice as large during QBOW as compared to QBOE for El Niño years without SSWs. Previous studies have never considered the combined influence of SSWs and QBO on ENSO teleconnections. It is interesting to note that Domeisen *et al* (2015) noted differences between the modeled and observed El Niño teleconnections during winters without SSWs and speculated that this was due to internal variability and limited observations. However, our study suggests that part of the differences between their model and observations could be due to the lack of a well represented QBO in their model.

The surface signatures of El Niño teleconnections are also very different during winters with and without SSWs. In agreement with modeling results of Ineson and Scaife (2009), 46LCAM5 simulates a positive SLP response in JFM over the polar cap during winters with SSWs, a feature that is not present during winters without SSWs. Ineson and Scaife (2009) also found a stronger Aleutian Low response during winters with SSWs compared to winters without SSWs. In 46LCAM5, we find a similar magnitude of the Aleutian low response in JFM for winters with and without SSWs; however, the response of the December–January average is stronger during winters with SSWs (not shown).

We found that QBOW winters intensify both the negative SLP anomaly in the North East Pacific as well as the positive SLP anomaly in the north-eastern Atlantic. Ineson and Scaife (2009) found a significant SLP anomaly over Northern Europe during winters without SSWs, and a high SLP anomaly in the eastern Atlantic; however their study did not consider the effects of the QBO. In our 10-member ensemble mean El Niño response, the NAO-like pattern is not apparent; however many of the ensemble members do show an NAO-like response, highlighting the influence of internal variability and sampling.

In summary, we have demonstrated that both SSWs and the phase of the QBO may influence El Niño teleconnection patterns in 46LCAM5, and that even with 8 events, El Niño composites are subject to considerable sampling fluctuations as a result of large internal variability. In our study we do not separate El Niño events into different 'flavors'; however that distinction could further influence our findings especially during winters without SSWs as suggested by Iza and Calvo (2015). The combined effects of SSWs and QBO on the El Niño teleconnections deserve more detailed studies; however this work suggests that the lack of explicit representation of these processes in GCMs may lead to an underestimate of the variability in El Niño teleconnection patterns.

Acknowledgments

We thank Julio Bacmeister for help with the development of the 46LCAM5 and Isla Simpson and Natalia Calvo for valuable discussions. We also thank the three anonymous reviewers for their thoughtful comments that have greatly improved this manuscript. The National Center for Atmospheric Research is sponsored by the National Science Foundation. L Sun is funded by a grant from the Office of Polar Programs at the National Science Foundation and by the Earth System Modeling program at the NOAA/Climate Program Office. NCEP Reanalysis data provided by the NOAA/OAR/ESRL PSD, Boulder, Colorado, USA, from their Web site at http://esrl.noaa.gov/psd/.

References

Alexander M A, Blade I, Newman M, Lanzante J R, Lau N C and Scott J D 2002 The atmospheric bridge: the influence of ENSO teleconnections on air–sea interaction over the global oceans *J. Clim.* **15** 2205–31

Baldwin M P *et al* 2001 The quasi-biennial oscillation *Rev. Geophys.* **39** 179–229

Baldwin M P and Dunkerton T J 2001 Stratospheric harbingers of anomalous weather regimes *Science* **294** 581–4

Branstator G W 2003 Remote response to tropical heating *Bull. Am. Meteorol. Soc.* **84** 1006–7

Butler A H, Polvani L M and Deser C 2014 Separating the stratospheric and tropospheric pathways of El Niño–Southern Oscillation teleconnections *Environ. Res. Lett.* **9** 024014

Calvo N, Giorgetta M A, Garcia-Herrera R and Manzini E 2009 Nonlinearity of the combined warm ENSO and QBO effects on the northern hemisphere polar vortex in MAECHAM5 simulations *J. Geophys. Res.* **114** D13109

Charlton A J and Polvani L M 2007 A new look at stratospheric sudden warmings. Part I. Climatology and modeling benchmarks *J. Clim.* **20** 449–69

Compo G P *et al* 2011 The twentieth century reanalysis project *Q. J. R. Meteorol. Soc.* **137** 1–28

Dennis J, Edwards J, Evans K, Guba O, Lauritzen P, Mirin A, St-Cyr A, Taylor M and Worley P 2012 CAM-SE: a scalable spectral element dynamical core for the community atmosphere model *Int. J. High Perform. Comput. Appl.* **26** 74–89

Deser C *et al* 2012 ENSO and pacific decadal variability in the community climate system model version 4 *J. Clim.* **25** 2622–51

Domeisen D I V *et al* 2015 Seasonal predictability over Europe arising from El Nino and stratospheric variability in the MPI-ESM seasonal prediction system *J. Clim.* **28** 256–71

Garfinkel C I, Butler A H, Waugh D W, Hurwitz M M and Polvani L M 2012 Why might stratospheric sudden warmings occur with similar frequency in El Niño and La Niña winters *J. Geophys. Res.* **117** D19106

Garfinkel C I and Hartmann D L 2007 Effects of the El Nino Southern Oscillation and the quasi-biennial oscillation on polar temperatures in the stratosphere *J. Geophys. Res.* **112** D19112

Garfinkel C I and Hartmann D L 2008 Different ENSO teleconnections and their effects on the stratospheric polar vortex *J. Geophys. Res.* **113** D18114

Garfinkel C I and Hartmann D L 2010 Influence of the quasi-biennial oscillation on the North Pacific and El Nino teleconnections *J. Geophys. Res.* **115** D20116

Garfinkel C I and Hartmann D L 2011a The influence of the quasi-biennial oscillation on the troposphere in winter in a hierarchy of models. Part I: simplified dry GCMs *J. Atmos. Sci.* **68** 1273–89

Garfinkel C I and Hartmann D L 2011b The influence of the quasi-biennial oscillation on the troposphere in winter in a hierarchy of models. Part 2: perpetual winter WACCM runs *J. Atmos. Sci.* **68** 2026–41

Garfinkel C I, Hartmann D L and Sassi F 2010 Tropospheric precursors of anomalous Northern Hemisphere stratospheric polar vortices *J. Clim.* **23** 3282–99

Gerber E P, Orbe C and Polvani L M 2009 Stratospheric influence on the tropospheric circulation revealed by idealized ensemble forecasts *Geoph. Res. Lett.* **36** L24801

Held I M, Mingfang T and Wang H 2002 Northern winter stationary waves: theory and modeling *J. Clim.* **15** 2125–44

Holton J R and Tan H 1980 The influence of the equatorial quasi-biennial oscillation on the global circulation at 50 mb *J. Atmos. Sci.* **37** 2200–8

Holton J R and Tan H-C 1982 The quasi-biennial oscillation in the northern hemisphere stratosphere *J. Meteorol. Soc. Japan* **60** 140–8

Horel J D and Wallace J M 1981 Planetary-scale atmospheric phenomena associated with the Southern Oscillation *Mon. Weather Rev.* **109** 813–29

Hurrell J W, Hack J J, Shea D, Caron J M and Rosinski J 2008 A new sea surface temperature and sea ice boundary dataset for the community atmosphere model *J. Clim.* **21** 5145–53

Ineson S and Scaife A A 2009 The role of the stratosphere in the European climate response to El Nino *Nat. Geosci.* **2** 32–6

Iza M and Calvo N 2015 Role of stratospheric sudden warmings on the response to central pacific El Nino *Geophys. Res. Lett.* **42** 2482–9

Jin D and Kirtman B P 2009 Why the Southern hemisphere ENSO responses lead ENSO *J. Geophys. Res.* **114** D23101

Kalnay E *et al* 1996 The NCEP/NCAR 40-year reanalysis project *Bull. Am. Meteorol. Soc.* **77** 437–71

Kidston J *et al* 2015 Stratospheric influence on tropospheric jet streams, storm tracks and surface weather *Nat. Geosci.* **8** 433–40

Manzini E *et al* 2006 He influence of sea surface temperatures on the northern winter stratosphere: ensemble simulations with the MAECHAM5 model *J. Clim.* **19** 3863–81

Neale R B *et al* 2012 Description of the NCAR community atmosphere model (CAM 5.0) *NCAR Technical Note NCAR TN 486* (www.cesm.ucar.edu/models/cesm1.0/cam/docs/description/cam5_desc.pdf)

Philander S G 1990 *El Nino, La Nina and the Southern Oscillation* (New York: Academic) p 293

Quadrelli R and Wallace J M 2004 A simplified linear framework for interpreting patterns of northern hemisphere wintertime climate variability *J. Clim.* **17** 3728–44

Richter J H, Bacmeister J T and Solomon A 2014a Effects of vertical resolution and non-orographic gravity wave drag on the simulated climate in the community atmosphere model, version 5 *J. Adv. Model. Earth Systems* **6** 357–83

Richter J H, Bacmeister J T and Solomon A 2014b On the simulation of the quasi-biennial oscillation in the community atmosphere model, version 5 *J. Geophys. Res.* **119** 3045–62

Richter J H, Sassi F and Garcia R R 2010 Towards a physically based gravity wave source parameterization in a general circulation model *J. Atmos. Sci.* **67** 136–56

Ropelewski C F and Halpert M S 1987 Global and regional scale precipitation patterns associated with the El Nino/Southern Oscillation *Mon. Weather Rev.* **115** 1606–26

Sassi F, Boville B, Kinnison D and Garcia R R 2005 The effects of interactive ozone chemistry on simulations of the middle atmosphere *Geophys. Res. Lett.* **32** L07811

Scaife A A *et al* 2014 Predictability of the quasi-biennial oscillation and its northern winter teleconnection on seasonal to decadal timescales *Geophys. Res. Lett.* **41** 1752–8

Scaife A A *et al* 2015 Seasonal winter forecasts and the stratosphere *Atmos. Sci. Lett.* (doi:10.1002/asl.598)

Sigmond M, Scinocca J F, Kharin V V and Shepherd T G 2013 Enhanced seasonal forecast skill following stratospheric sudden warmings *Nat. Geosci.* **6** 98–102

Thompson D W J and Wallace J M 2001 Regional climate impacts of the northern hemisphere annular mode *Science* **293** 85–9

Tippett M K and Barnston A G 2008 Skill of multimodel ENSO probability forecasts *Mon. Weather Rev.* **136** 3933–46

Trenberth K E, Branstator G W, Karoly D, Kumar A, Lau N C and Ropelewski C 1998 Progress during TOGA in understanding and modeling global teleconnections associated with tropical sea surface temperatures *J. Geophys. Res.* **103** 14291–324

Tripathi O P *et al* 2014 The predictability of the extra- tropical stratosphere on monthly timescales and its impacts on the skill of tropospheric forecasts *Q. J. R. Meteorol. Soc.* **141** 987–1003

Uppala S *et al* 2005 The ERA-40 reanalysis. *Q. J. Roy. Meteorol. Soc.* **131** 2961–3012

Wallace J M and Gutzler D S 1981 Teleconnections in the Geopotential height field during the northern hemisphere winter *Mon. Weather Rev.* **109** 784–812

Zhang G J and McFarlane N A 1995 Sensitivity of climate simulations to the parameterization of cumulus convection in the Canadian climate centre general circulation model *Atmos. Ocean* **3** 407–46